# Experimental and Computational Studies of Trialkylaluminum and Alkylaluminum Chloride Reactions with Silica

**Jonathan P. Blitz,*,† Richard E. Diebel,† Carol A. Deakyne,‡ Jeannine M. Christensen,† and Vladimir M. Gun'ko§**

*Department of Chemistry, Eastern Illinois University, Charleston, Illinois 61920, Department of Chemistry, University of Missouri at Columbia, Columbia, Missouri, and Institute of Surface Chemistry, 17 General Naumov Street, 03164 Kiev, Ukraine*

*Received: July 8, 2004; In Final Form: December 13, 2004*

Reactions of trimethylaluminum, triethylaluminum, and diethylaluminum chloride and ethylaluminum dichloride with silica gel have been studied experimentally by infrared spectroscopy and elemental analysis. The silica gel was subjected to different pretreatments to alter surface functionalities prior to reaction. In all cases the extent of surface modification reaction follows the trend unmodified > 600 °C pretreated > hexamethyldisilazane (HMDZ) pretreated > 600 °C/HMDZ pretreated. All of the aluminum compounds studied completely react non-hydrogen-bonded silanols, while also reacting with hydrogen-bonded silanols and siloxanes. Primarily monomeric surface species result from the surface modification reaction. Ethylaluminum chlorides preferentially react with silanols through cleavage of the Al−C bond rather than the Al−Cl bond. Singly bonded Si(s)−O−$AlCl_2$ surface species are readily synthesized by reaction of ethylaluminum dichloride with HMDZ-pretreated silica gel. Bridged bonded $(Si(s)-O)_2$−AlCl surface species are readily synthesized by reaction of diethylaluminum chloride with HMDZ-pretreated silica gel. Computational ab initio studies of the cluster $Si_4O_6(OH)_4$ as a model to study the reaction of monomeric and dimeric methylaluminum dichloride with a silica silanol are also described. Comparison of the potential energy surface (PES) of monomer and dimer indicates that the energetics favor monomer reaction, consistent with experimental results. The energy cost in the dimer reaction is primarily from cleavage of a bridged Al−Cl bond upon adsorption. This does not occur when the monomer adsorbs. A comparison of the PES for the two reaction pathways resulting from cleavage of either an Al−Cl or Al−C bond indicates that while the former reaction is slightly kinetically favored ($E_a$ = 23.1 kJ/mol for Al−Cl bond cleavage versus $E_a$ = 31.1 kJ/mol for Al−C bond cleavage), the latter is strongly thermodynamically favored with an overall free energy difference between the two reaction pathways of 135 kJ/mol favorable to Al−C bond cleavage. These reactions are thermodynamically controlled.

## Introduction

The reactions of aluminum alkyls with silica have been studied by researchers with a variety of interests ranging from catalysis to materials science. Regardless of the application, a fundamental knowledge of the nature of these reactions remains important for future development. Using trimethylaluminum (TMA) as the most studied example,[1−15] there is general agreement that TMA reacts with a surface silanol, releasing methane (eq 1).

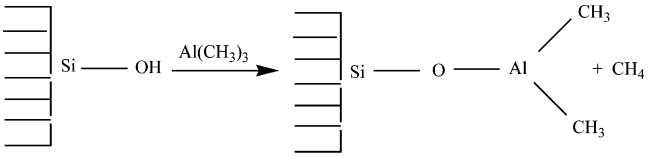


(1)

TMA can also react with surface siloxanes, resulting in a methyl transfer from aluminum to a surface-bound silicon (eq 2).

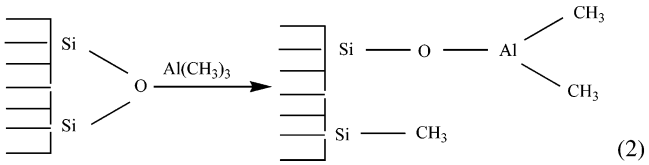


(2)

The singly bonded aluminum species resulting from reaction of a surface silanol may undergo further reaction with either an adjacent silanol or a siloxane to form what may be termed a bridged bonded compound.

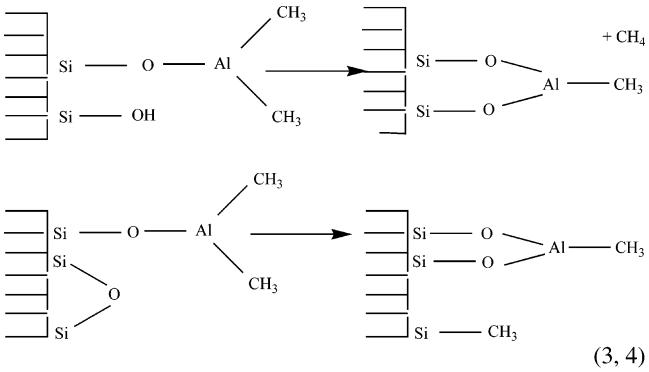


(3, 4)

* To whom correspondence should be addressed; e-mail jpblitz@eiu.edu.
† Eastern Illinois University.
‡ University of Missouri at Columbia.
§ Institute of Surface Chemistry.

10.1021/jp040483j CCC: $30.25 
Published on Web 03/05/2005

Our interest has been to investigate how different silica surface groups react with a variety of reagents in an attempt not only to understand how these reactions occur but also to manipulate the modified surface structure.[16,17] To this end a set of silicas has been prepared to compare their reactivity and resulting modified surface structure. In this model four different silica gels are studied: (1) unmodified silica gel containing nonhydrogen-bonded silanols, hydrogen-bonded (adjacent) silanols, and siloxanes; (2) 600 °C pretreated silica gel containing nonhydrogen-bonded silanols and siloxanes; (3) hexamethyldisilazane (HMDZ) modified silica containing hydrogen-bonded silanols and siloxanes; and (4) 600 °C + HMDZ modified silica gel containing only, or at least predominantly, surface siloxanes.

In this work a series of ethylaluminum chloride reactions with the different pretreated silica gels have been investigated. These systems are of interest since the aluminum compound can react through the loss of either a chloro or an ethyl group, resulting in different surface species. This is shown in eqs 5 and 6 for ethylaluminum dichloride.

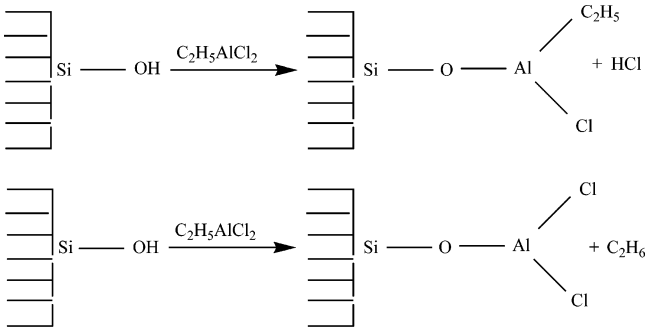


(5, 6)

If ethylaluminum dichloride reacts with Al−Cl bond cleavage, then an aluminum alkyl group can remain on the modified surface. In heterogeneous olefin polymerization catalysis this $Al-C_2H_5$ group can reduce a catalytically active metal species, altering its behavior. In contrast, if ethylaluminum dichloride reacts with $Al-C_2H_5$ bond cleavage, only Al−Cl bonds remain on the surface. This type of cleavage may provide an alternative means to synthesize solid acid catalysts for alkylation, isomerization, or cracking reactions, which often utilize $AlCl_3$ to modify the silica support. Previous workers have suggested that the reaction takes place preferentially with loss of ethane.[18−20] Results presented in this report lead to the same conclusion, along with additional insight into the nature of the surface groups reacted and surface species formed. Furthermore, the reasons for the experimentally determined reaction path are explored in some detail by use of ab initio quantum chemical techniques.

## Experimental and Computational Details

**Materials.** Davison 948 silica gel (W. R. Grace, BET surface area ~275 $m^2/g$) was pretreated in four ways prior to reaction: (1) evacuated (0.1 mmHg) for 5 h at 225 °C to remove surface-adsorbed water (termed unmodified silica); (2) reacted with hexamethyldisilazane as previously described,[21] followed by evacuation for 5 h at 225 °C; (3) heated for 5 h at 600 °C in air (termed 600 °C silica); and (4) first heated for 5 h at 600 °C in air, then reacted with HMDZ (5 mmol/g of silica in toluene slurry) for 3 h at room temperature, then filtered and evacuated for 2 h at 225 °C (termed 600 °C/HMDZ silica).

Hexanes (EM Science), heptane (Aldrich), and toluene (Mallinckrodt) were dried under argon with $CaH_2$ for a minimum of 12 h prior to use. Trimethylaluminum (TMA), triethylaluminum (TEAL), diethylaluminum chloride (DEAC), and ethylaluminum dichloride (EADC) were obtained from Aldrich as hexane solutions and used as received. **Caution:** Aluminum alkyls are pyrophoric, and precautions must be taken to isolate these compounds from oxygen and moisture. $CaH_2$ reacts very exothermically with water and alchohols.

**Experimental Methods.** All reactions were performed in a controlled atmosphere glovebox (VAC) with water and oxygen concentrations less than 5 ppm. One gram of silica gel was slurried in 50 mL of solvent. Reactions involving HMDZ, 600 °C, and 600 °C/HMDZ silicas utilized 5 mmol of organoaluminum compound, whereas reactions involving unmodified silica were carried out with 10 mmol of organoaluminum compound. The reactions were allowed to proceed for 1 h with occasional swirling. The solution was then decanted and the silica was washed 4 times with 20 mL portions of solvent. The modified silica was then evacuated for 2 h prior to permanent storage in the glovebox.

Infrared spectra were obtained with a Nicolet 7199 FT-IR spectrometer purged with dry air and equipped with a mercury−cadmium−telluride (MCT) detector. Spectra were obtained at 4 $cm^{-1}$ nominal resolution with coaddition of 128 scans. Samples were prepared in an inert atmosphere glovebox with a 10% (w/w) dispersion of silica in ground, dried KCl. A controlled atmosphere diffuse reflectance cell (Harrick Scientific) was utilized to minimize sample exposure to atmospheric water and oxygen. This cell was modified to permit optimum sample height adjustments for quantitative work.[22,23]

Inductively coupled plasma (ICP) for elemental analysis was accomplished with a Leeman Laboratories PS-1000. Silica samples were fused with a 4:1 mixture of sodium carbonate/lithium tetraborate and dissolved in 10% nitric acid. Analysis wavelengths used were 251.611 nm for Si and 308.215 nm for Al.

Surface silanol concentrations were determined by reaction of the silica gels with a 3.0 M ether solution of methylmagnesium iodide. Reactions were carried out in a sealed vial connected to a manifold equipped with a pressure transducer. Reproducible measurements were obtained on all samples except HMDZ silica, so the surface silanol concentration of this material was estimated. The silanol concentration of unmodified silica gel, and carbon analysis (Galbraith Laboratories, Knoxville, TN) of HMDZ silica provides the required data. Given that 3 moles of carbon react with 1 mole of silanol, subtraction of the carbon data from the silanol content of unmodified silica provides the estimate for the silanol content of HMDZ silica.

**Theoretical Methods.** Standard ab initio calculations were carried out with use of the Gaussian 98 set of programs.[24] Fully optimized structures were obtained at the HF/6-31G(d,p) level of theory. Electron correlation was taken into account by evaluating MP2(fc)/6-31G(d,p) single-point energies for each equilibrium structure. The energies have not been corrected for basis-set superposition errors (BSSE). Zero-point vibrational energies (ZPEs) and thermal temperature corrections were derived from vibrational frequencies scaled by the usual factor of 0.8929.[25] The vibrational frequencies were also utilized to confirm minima and maxima along the reaction pathways.

Cluster and crystal models of silica and adsorption complexes have been utilized for ab initio calculations.[26−42] The cluster $Si_4O_6(OH)_4$ **1** has been chosen to model a fragment of the silica surface with a terminal silanol group. This model cluster was also utilized by Molotovshchikova et al.[43] in their PM3 study of the enthalpies of complex formation of $Al(CH_3)_3$ and $Al(C_2H_5)_3$ with various active centers of the silica surface. On

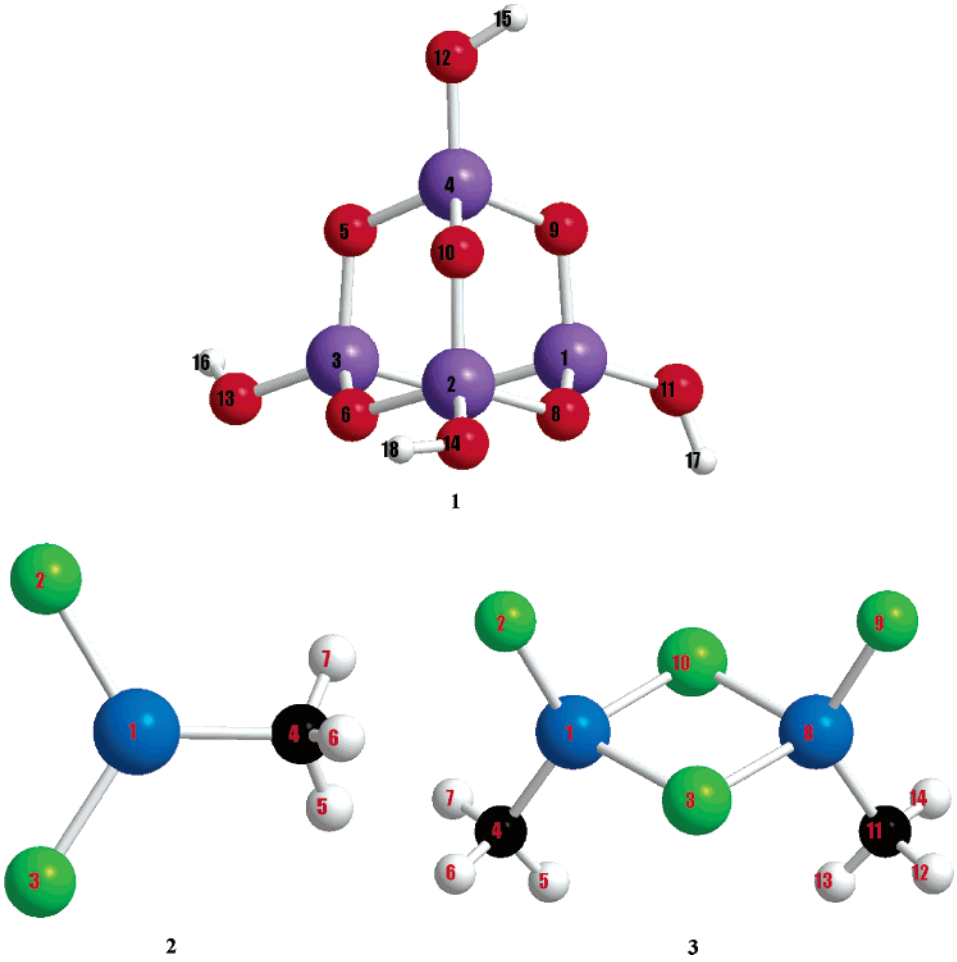


**Figure 1.** Reactants $Si_4O_6(OH)_4$ (**1**), $AlCl_2CH_3$ (**2**), and $Al_2Cl_4(CH_3)_2$ (**3**) with atomic numbering used throughout the text.

the basis of our discussion below concerning the relative reactivity of TMA and TEAL, calculations were performed on the simpler $AlCl_2CH_3$ system rather than $AlCl_2C_2H_5$. This substitution also reduces any preference for loss of alkyl vs Cl due to steric strain. Reaction of both the monomer $AlCl_2CH_3$ **2** and dimer $Al_2Cl_4(CH_3)_2$ **3** with a free silanol group on the silica surface have been considered. Compounds **1**−**3** are depicted in Figure 1 with the atomic numbering that is used throughout the text.

Two reaction pathways, that is, loss of HCl and loss of $CH_4$, have been examined for each set of reactants. The overall reactions are given in eqs 7−10:

$$AlCl_2CH_3 + Si_4O_6(OH)_4 \rightarrow Si_4O_7(OH)_3{-}AlClCH_3 + HCl \quad (7)$$

$$AlCl_2CH_3 + Si_4O_6(OH)_4 \rightarrow Si_4O_7(OH)_3{-}AlCl_2 + CH_4 \quad (8)$$

$$Al_2Cl_4(CH_3)_2 + Si_4O_6(OH)_4 \rightarrow Si_4O_7(OH)_3{-}Al_2Cl_3(CH_3)_2 + HCl \quad (9)$$

$$Al2Cl_4(CH_3)_2 + Si_4O_6(OH)_4 \rightarrow Si_4O_7(OH)_3{-}Al_2Cl_4CH_3 + CH_4 \quad (10)$$

The first step for each pathway involves formation of the prereaction complex between the two reactant molecules. For reactions 7 and 9, the pathway is subdivided into two further steps. In the second step the prereaction complex is converted into a hydrogen-bonded complex in which HCl interacts with an adjacent oxygen atom of a siloxane group. The third step involves the dissociation of the hydrogen-bonded complex to form products. For reactions 8 and 10, the prereaction complex breaks down directly to products. The transition state for the second step in each of these reaction schemes has also been identified. The complete reaction schemes for the two pathways are generalized in eqs 11 and 12, where $m = 2, 4$ and $n = 1, 2$:

$$Al_nCl_m(CH_3)_n + Si_4O_6(OH)_4 \rightarrow Si_4O_6(OH)_4{-}Al_nCl_m(CH_3)_n \rightarrow TS \rightarrow ClH\cdots Si_4O_7(OH)_3{-}Al_nCl_{m-1}(CH_3)_n \rightarrow Si_4O_7(OH)_3{-}Al_nCl_{m-1}(CH_3)_n + HCl \quad (11)$$

$$Al_nCl_m(CH_3)_n + Si_4O_6(OH)_4 \rightarrow Si_4O_6(OH)_4{-}Al_nCl_m(CH_3)_n \rightarrow TS \rightarrow Si_4O_7(OH)_3{-}Al_nCl_m(CH_3)_{n-1} + CH_4 \quad (12)$$

Natural bond orbital (NBO) analysis[44] of the Hartree−Fock (HF) molecular orbitals has been utilized to investigate the influence of hyperconjugative effects on the geometrical parameters and stabilities of the complexes. Analyses of the charge distributions and charge-transfer processes were performed with the natural charges obtained from the NBO analysis, with charges obtained from a Mulliken population analysis,[45] and with charges fit to the electrostatic potential according to the Merz−Singh−Kollman scheme.[46] Since the trends are similar for all three methods, only the NBO results are reported.

Finally, calculations with consideration of solvation effects were performed for the monomer reactions. The solvation model SM5.42R/6-31G(d)[47] (GAMESOL version 3.1 with addition of some parameters for Si and Al) was applied to the geometry of the prereaction complex and transition state found for the gas phase.

## Results and Analysis

**A. Extent of Reaction: Experimental.** Results of the extent of surface modification reaction, measured by ICP as millimoles of Al/gram of $SiO_2$, are provided in Table 1. In all cases the extent of reaction follows the trend unmodified > 600 °C > HMDZ > 600 °C/HMDZ silica. Since unmodified silica gel has the highest surface silanol concentration (Table 1), it is not surprising that the largest amount of alkylaluminum compound reacts with this material. Similarly, the 600 °C/HMDZ silica possesses little or no detectable surface silanols, so the least amount of alkylaluminum reacts with silica gel pretreated in this way.

The aluminum content of 600 °C/HMDZ silica gel should be a reliable indicator of the extent of alkylaluminum reaction with surface siloxanes, since it is believed that all or nearly all the surface-bound aluminum content of 600 °C/HMDZ silica gel is from siloxane reaction. With this in mind, for example, 0.41 mmol of Al/g of $SiO_2$ is present on the modified silica gel when triethylaluminum is reacted with 600 °C/HMDZ silica. In comparison, triethylaluminum-reacted 600 °C silica gives a surface aluminum concentration of 1.20 mmol/g. The surface silanol concentration of 600 °C silica gel is found to be approximately 0.6 mmol/g, and as seen by infrared spectroscopy (vide supra), the surface silanols are completely reacted. The remaining 0.6 mmol of Al/g found on TEAL-reacted 600 °C silica is reacted with surface siloxanes (assuming 1 Al reacted/silanol). The apparently greater extent of siloxane reaction on 600 °C silica with respect to HMDZ/600 °C silica is observed for all of the reactants studied. One possible explanation for this result is that the heat of reaction of alkylaluminum with surface silanols on 600 °C silica may result in additional surface siloxane reaction as compared to 600 °C/HMDZ silica, where no silanols are present. The ab initio calculations presented below will provide data on the thermochemistry of these reactions.

*Aluminum Dimers.* It is also possible that the approximately 2/1 Al/SiOH ratio seen on 600 °C silica is a result of reaction of aluminum dimers with silica. It has been reported that TEAL in hexanes is >90% dimerized,[48] as are the ethylaluminum chlorides at room temperature.[49] Thus surface species may be more accurately depicted as dimeric.

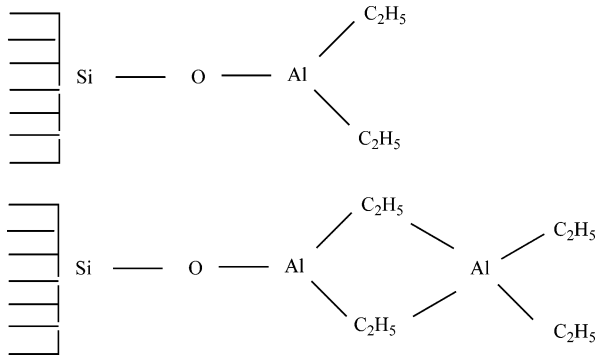


The evidence seems to favor monomeric species formation since these alkylaluminum compounds apparently react with surface siloxanes, as shown by previous workers[1,8,12−14] and the results reported here with 600 °C/HMDZ silica. If primarily surface dimers were present, there would be no excess surface-bound aluminum to explain the siloxane bond reaction. A mixture of monomeric and dimeric surface species is possible, however, and may explain some, though not all, of the excess surface-bound alkylaluminum with respect to silanol concentration. The possibility that both monomeric and dimeric species may exist has been previously explored for similar compounds.[11,50]

**TABLE 1: Extent of Reaction of Aluminum Compounds[a] with Four Different Types of Pretreated Silica Gels**

| silica gel type | TEAL loading (mmol of Al/g of $SiO_2$) | DEAC loading (mmol of Al/g of $SiO_2$) | EADC loading (mmol of Al/g of $SiO_2$) | TMA loading (mmol of Al/g of $SiO_2$) | SiOH concn (mmol of SiOH/g of $SiO_2$) |
|---|---|---|---|---|---|
| unmodified | 1.80 | 1.70 | 1.96 | 2.18 | 1.7 |
| 600 °C | 1.20 | 1.20 | 1.26 | 1.40 | 0.6 |
| HMDZ | 0.57 | 0.48 | 1.07 | 0.73 | 0.8 |
| 600 °C/HMDZ | 0.41 | 0.33 | 0.57 | 0.47 | 0 |

[a] Triethylaluminum (TEAL), diethylaluminum chloride (DEAC), ethylaluminum dichloride (EADC), and trimethylaluminum (TMA) were evaluated. Silanol concentrations are also shown.

*Singly vs Doubly Bonded Surface Aluminum Species.* Since the work reported by Bartram et al.,[8] the extent to which singly bonded surface aluminum species exist on TMA-modified silica has been debated. Assuming monomeric surface species on 600 °C silica gel, with 1.40 mmol of Al/g of silica reacted and a silanol concentration of 0.6 mmol/g, then 0.8 mmol/g TMA is presumed to have reacted with siloxanes. If only singly bonded species exist on this silica (eqs 1 and 2), then 78% of methyl groups remaining are attached to Al. The remainder exist as $Si-CH_3$ groups. If the former species undergo further reaction to form bridged bonded compounds (eq 4), then $Al-CH_3$ groups comprise 39% and $Si-CH_3$ groups 61% of adsorbed methyl groups. Work by Anwander et al.[12] on TMA-modified silica prepared in a way similar to this work found 71% $Al-CH_3$ and 29% $Si-CH_3$ groups. These data support the contention of others[12,13] that singly bonded aluminum compounds do exist on these modified surfaces and may be the predominant species on 600 °C silica gel under these conditions.

*Ethyl Group Substitution.* A comparison between the reactivities of trimethyl and triethylaluminum was made (Table 1). In all cases trimethylaluminum reactions result in a slightly greater aluminum surface concentration, indicating a larger extent of reaction compared to triethylaluminum. It has been proposed that the extent of trialkylaluminum reaction can be affected by the size of the alkyl group,[11] thus differences in the extent of reaction are interpreted as primarily a steric effect. Previous work on heat-treated trimethylaluminum-reacted silicas suggest surface aluminum loadings of 2.8−3.2 Al/nm$^2$. These data are in general agreement with the entry in Table 1 for trimethylaluminum-reacted 600 °C pretreated silica gel, which corresponds to 3.3 Al/nm$^2$.

The substitution of one or two ethyl groups by chloro groups reveals an interesting trend with respect to alkylaluminum reactivity with the different silicas. Given a relative standard deviation for the values in Table 1 of approximately 10%, there is little difference in the overall reactivity of the three organoaluminum compounds studied. However, the relative extent of reaction that occurs with HMDZ silica is striking. Approximately twice the amount of aluminum (1.07 mmol/g) is bonded to the surface as a result of ethylaluminum dichloride reaction than as a result of diethylaluminum chloride (0.48

**SCHEME 1: Reactions of $TiCl_4$ and $(C_4H_9)_2Mg$ with Hydrogen-Bonded Silanols**

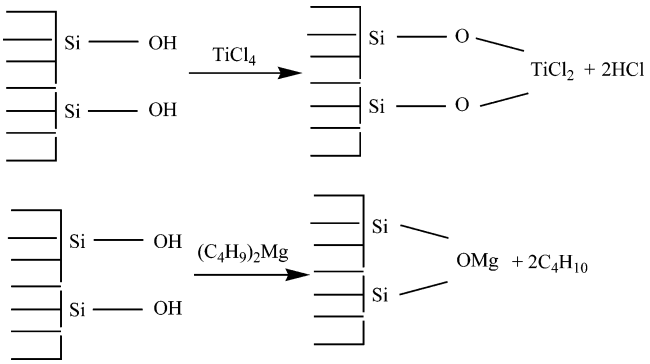


**SCHEME 2: Proposed Reaction Products of Ethylaluminum Chloride Reactions with Hydrogen-Bonded Silanols**

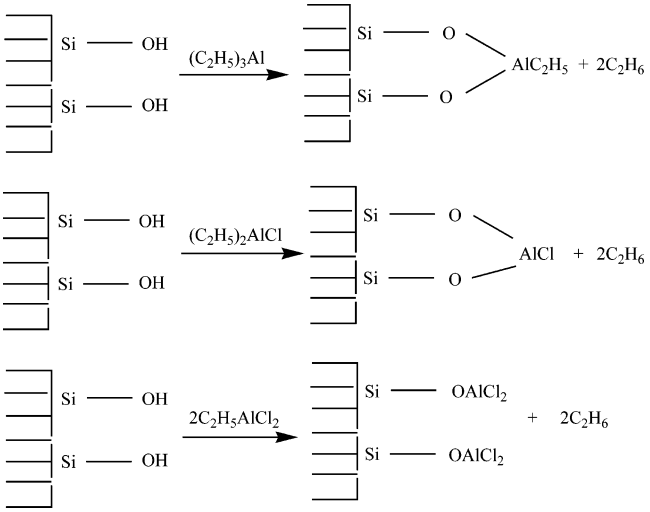


mmol/g) or triethylaluminum (0.57 mmol/ g) reaction. Since this trend is not seen for the other pretreated silicas, it is concluded that ethylaluminum dichloride is not inherently more reactive but reacts differently with HMDZ silica compared to the other two reactants.

To assess how these different alkyl aluminum compounds react with HMDZ silica, it is noted that this surface possesses predominantly hydrogen-bonded silanols. It has been previously shown[16,17] that both $TiCl_4$ and dibutylmagnesium react with HMDZ silica to form bridged bonded surface species as shown in Scheme 1.

In these cases 1 mol of titanium or magnesium compound reacts with 2 mol of hydrogen-bonded silanols. Analogously, the elemental analysis data can be rationalized if both triethylaluminum and diethylaluminum chloride react in a 1:2 mole ratio with respect to surface silanols, whereas ethylaluminum dichloride reacts in a 1:1 mole ratio. The proposed reaction schemes are illustrated below in Scheme 2.

**B. Reaction Products: Experimental.** Infrared spectral results of these materials provide some additional insight into the reactions of these compounds with the various silica surface groups. Infrared spectra of unmodified and 600 °C silica gel, before and after reaction with triethylaluminum, diethylaluminum chloride, and ethylaluminum dichloride, are shown in Figures 2 and 3, respectively. Prior to reaction, the unmodified and 600 °C silica gels exhibit a sharp absorbance at approximately 3745 $cm^{-1}$ from non-hydrogen-bonded silanols. The broad peak ranging from 3700 to 3200 $cm^{-1}$ in the unmodified

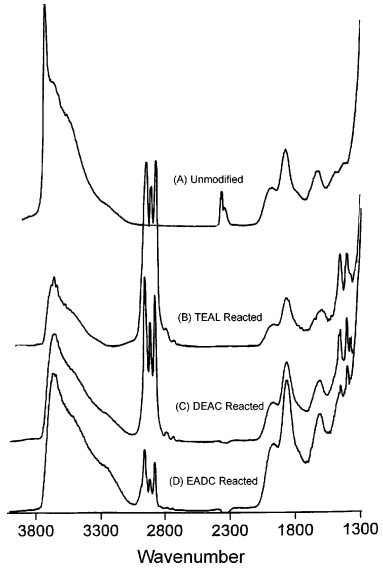


**Figure 2.** Infrared spectra of unmodified silica gel before and after reaction with ethylaluminum chlorides.

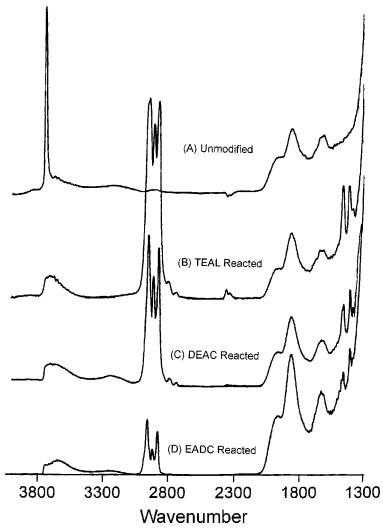


**Figure 3.** Infrared spectra of 600 °C silica gel before and after reaction with ethylaluminum chlorides.

silica gel is from hydrogen-bonded silanols in various hydrogen-bonding environments. These silanols are condensed as a result of 600 °C thermal treatment. Si−O−Si overtone and combination bands are seen at approximately 1800 and 1600 $cm^{-1}$, respectively, in all cases. After reaction with any of the alkylaluminum compoounds, the non-hydrogen-bonded silanol band disappears, indicating these silanols are completely reacted. Assuming that reaction of non-hydrogen-bonded silanols results in a singly attached surface aluminum species, analogous to what has been previously reported for $TiCl_4$[16] and dibutylmagnesium,[17] two possible pathways exist for diethylaluminum chloride and ethylaluminum dichloride. These reagents can react either with cleavage of the Al−Cl bond, releasing HCl, or with cleavage of the Al−C bond, releasing $C_2H_6$. For triethylaluminum reaction there will be two ethyl groups remaining per surface-bound aluminum. If diethylaluminum chloride reacts with loss of HCl there will also be two ethyls per aluminum, whereas if this reagent reacts with loss of $C_2H_6$ there will be only one ethyl per aluminum (Scheme 3).

Similarly, if ethylaluminum dichloride reacts with loss of HCl there will exist one ethyl group per aluminum; however, if $C_2H_6$

**SCHEME 3: Possibilities of Diethylaluminum Chloride Reacting with Non-Hydrogen-Bonded Silanols**

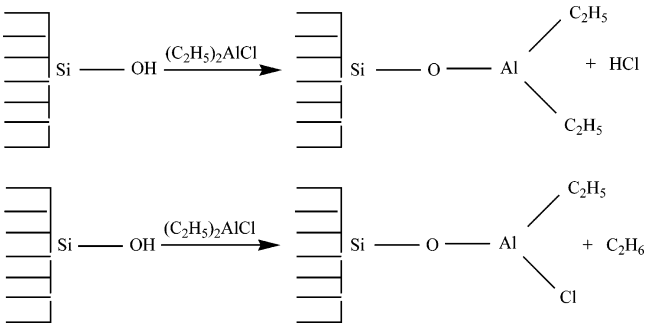


**TABLE 2: CH/Al Ratio of Aluminum Compounds Reacted with Unmodified and 600 °C Silica Gels**

| silica gel type | reactant | CH/Al ratio |
|---|---|---|
| unmodified | TEAL | 0.35 |
| unmodified | DEAC | 0.19 |
| unmodified | EADC | 0.07 |
| 600 °C | TEAL | 0.38 |
| 600 °C | DEAC | 0.23 |
| 600 °C | EADC | 0.08 |

[a] Triethylaluminum (TEAL), diethylaluminum chloride (DEAC), and ethylaluminum dichloride (EADC) were evaluated.

is liberated then no ethyl groups will remain as a result of this reaction (see Introduction).

To determine whether the ethylaluminum chlorides react with loss of HCl or $C_2H_6$, a combination of Fourier transform infrared (FT-IR) and ICP elemental analysis data was analyzed. In Table 2 the CH/Al ratio is provided for unmodified and 600 °C modified silica gels after reaction with triethylaluminum, diethylaluminum chloride, and ethylaluminum dichloride. The ratio of an integrated CH bending band (1504−1434 $cm^{-1}$) to a Si−O−Si combination band centered at approximately 1860 $cm^{-1}$ used as an internal standard was first obtained. The resulting unitless number, which correlates with the amount of CH present on the modified silica gels, was then normalized to the aluminum concentration (millimoles per gram) found by ICP. This value is designated as the CH/Al ratio. If the reaction occurs with loss of HCl, the CH/Al ratio will be the same for triethylaluminum and diethylaluminum chloride modified silicas. In contrast, the CH/Al ratio for diethylaluminum chloride will be half that of triethylaluminum if the reaction occurs with loss of $C_2H_6$. The data clearly indicate that ethane loss is the predominant mode of reaction, in agreement with the contention of previous workers.[18−20] These results suggest a means to synthesize Al−Cl surface-bound species that are either singly or bridged bonded. To form a singly bonded species, HMDZ-silica is reacted with ethylaluminum dichloride, whereas a bridged bonded species is synthesized by reaction of HMDZ-silica with diethylaluminum chloride (Scheme 2), which possesses two reactive alkyl groups. Evidence for the formation of the bridged bonded species is obtained from the CH/Al ratio of the DEAC-reacted HMDZ-silica (0.07), which is significantly less than the value for DEAC-reacted 600 °C or unmodified silica (Table 2).

The nonzero CH/Al ratios associated with the materials derived from reaction of silica gels with EADC- or DEAC-reacted HMDZ-silica is readily explained. It may be that a minor reaction does occur with HCl loss or, more likely, detection of surface-bound CH groups from reaction with siloxanes is seen. Support for the latter explanation comes from the result that each alkylaluminum reacts to a significant extent with HMDZ/600 °C silica, where siloxanes are the primary surface species present.

The fact that ethylaluminum chlorides preferentially react with ethane loss is surprising, since $AlCl_3$ has often been reported to readily modify silica surfaces.[2,3,51−54] Studies with ab initio quantum chemical techniques were therefore undertaken in an attempt to understand this behavior.

**C. Reaction Pathways: Computational.** The stationary point structures for the reactions of $AlCl_2CH_3$ with $Si_4O_6(OH)_4$ (reactions 7 and 8) are illustrated in Figure 4. The analogous structures for the reactions of $Al_2Cl_4(CH_3)_2$ with $Si_4O_6(OH)_4$ (reactions 9 and 10) are illustrated in Figure 5. Computed molecular properties are given in Table 3, and relative energies, enthalpies, and free energies are collected in Table 4. Selected geometrical parameters are reported in the Supporting Information (Table S1).

The molecular properties compiled in Table 3 are related to the charge-transfer processes in the equilibrium complexes. The partial charges on the acceptor aluminum and donor oxygen atoms, $q_{Al1}$ and $q_{O12}$, respectively, are the natural charges obtained from the NBO analysis of the Hartree−Fock molecular orbitals. The second-order perturbation approach was used to evaluate energies of hyperconjugative interactions [$\Delta E^{(2)}$(donor → acceptor)].[55] Frequently more than one lone pair on a particular atom overlaps with a given unfilled natural bond orbital. In those cases, the second-order perturbation energy reported in Table 3 is the sum of the NBO interaction energies for the lone pairs delocalizing into the unfilled orbital. In all of the prereaction, hydrogen-bonded, and product complexes, the Lewis NBOs describe about 99.0% of the total electron density, with the majority of the non-Lewis density in the valence-shell antibonds (0.8%). The non-Lewis NBOs with highest occupancy are the $p_{z,Al1}$ (0.15e) and $\sigma_{Si-O}^*$ (∼0.08e) orbitals.

Kudo and Gordon[56] have shown that, for the first step of the hydrolysis of $RSiCl_3$ (R = H, Me, *t*-Bu, and Ph), bond distances in the transition-state structures can vary by as much as 0.1−0.2 Å at the HF/6-31G(d) and MP2/6-31G(d) levels of theory. Nevertheless, trends in structural changes are reproduced at the HF level. Anticipating similar results for the reactions examined in this work (eqs 7−10), we have focused primarily on structural differences in the discussion below.

One of the several structural features notable for molecules **1**−**15** is that the framework of the $Si_4O_6(OH)_4$ surface model is quite rigid. It is primarily the geometrical parameters of the Si4−O12−H15 donor moiety and the O−Si−O−H dihedral angles that show the most flexibility (e.g., O5−Si3−O13−H16; Table S1). In some cases, rotation about the latter Si−O bond is large enough to reverse the sign of the dihedral angle in **1**. The rotations accommodate the bulky reactant moiety and/or the hydrogen-bonded hydrochloric acid (Figures 4 and 5). Within the cluster ring, the greatest changes occur for the Si4−O bond lengths (≤0.025 Å) and O−Si4−O angles (≤5°) in the prereaction or hydrogen-bonded complexes.

*Prereaction Complexes*. Although the geometry about aluminum is more pyramidal in prereaction complex **4** than in reactant **2**, it is well distorted from tetrahedral (Figure 4 and Table S1). The two chlorine atoms and methyl group are arranged about aluminum in a fashion that is close to trigonal. The Cl−Al−X angles have decreased by only 2−3° from their values in **2**. The relevant hydroxyl hydrogen atom H15 is eclipsed to chlorine atom Cl2, with a dihedral angle of −5.2°. A lone pair on oxygen is coordinated to the empty $p_z$ orbital of aluminum, forming an Al1−O12 bond that is ∼0.3 Å longer

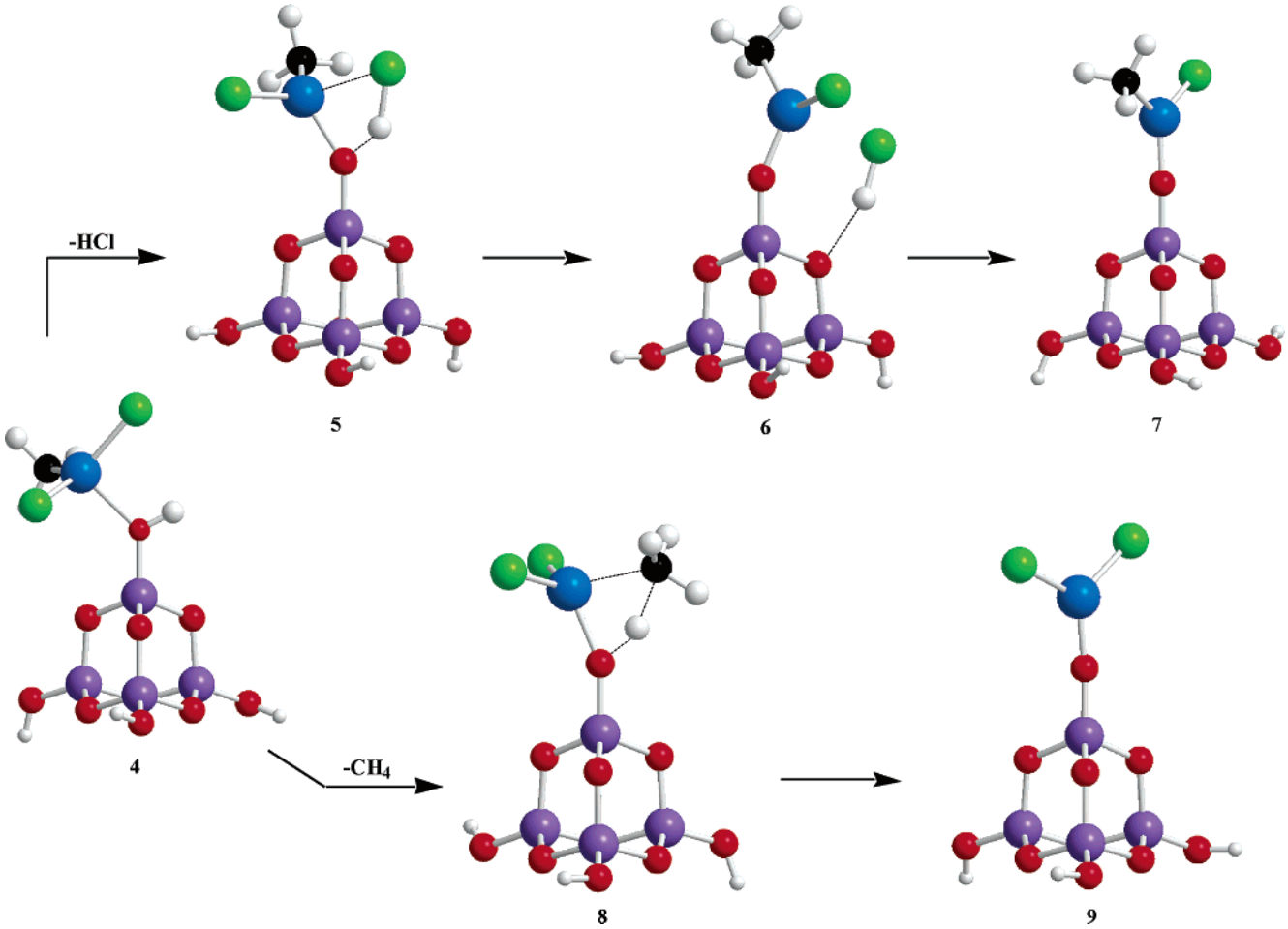


**Figure 4.** Stationary point structures of the two possible reaction pathways for the reaction of $Si_4O_6(OH)_4$ (**1**) with $AlCl_2CH_3$ (**2**).

than in the product complexes and O12−Al1−X bond angles that average 99.7°. Xu et al.[57] found similar structural features in their DFT study of $H_7AlSi_3O_4Cl_2$, $H_9AlSi_4O_7Cl_2$ and $H_7AlSi_3O_8Cl_2$ to characterize the acidity of the solid acid catalyst $(SG)_nAlCl_2$. Consistent with a limited Al1−O12 overlap is the small intermolecular charge transfer of 0.0865e and, by comparison with similar donor−acceptor complexes,[58] the relatively modest second-order perturbation energy $\Delta E^{(2)}(n_{O12} \rightarrow p_{z,Al1})$ of 241.9 kJ/mol (Table 3). Other, more minor contributions to the Al1−O12 interaction are the $\sigma_{Si4-O12} \rightarrow p_{z,Al1}$ and $\sigma_{O12-H15} \rightarrow p_{z,Al1}$ hyperconjugations.

When dimer reactant **3** forms the donor−acceptor complex **10**, the Al−Cl bond between the acceptor aluminum atom Al1 and the bridged chlorine atom Cl10 is broken (Figure 5 and Table S1). Such a bond dissociation was also reported by Fraile et al.[59] in their HF/6-31G(d) study of the interaction between formaldehyde and $Al_2Cl_2(CH_3)_4$. With this dissociation, the environment around the acceptor Al1 atom is similar in **4** and **10**. Nevertheless, the Al1−O12 bond length is shorter in **10** than in **4** (2.008 vs 2.035 Å). Examining the data in Table 3 shows that the energy contributions of the $\sigma_{Si4-O12} \rightarrow p_{z,Al1}$ and $\sigma_{O12-H15} \rightarrow p_{z,Al1}$ interactions, $\Delta E^{(2)}(\sigma_{Si4-O12} \rightarrow p_{z,Al1})$ and $\Delta E^{(2)}(\sigma_{O12-H15} \rightarrow p_{z,Al1})$, respectively, are larger for **10** than for **4**. Also consistent with the somewhat stronger donor−acceptor bond in **10** are the enhanced electrostatic attraction between the O12 and Al1 atoms and the enhanced intermolecular charge transfer of 0.0953e (cf. Table 3 and ref 58). Two other sets of geometrical parameters of interest are the distances between the hydroxyl hydrogen H15 and eclipsed chlorine Cl2 atoms of 2.745 Å (**4**) vs 2.870 Å (**10**) and the distances between the H15 and carbon C4 atoms of 3.757 Å (**4**) vs 3.964 Å (**10**).

Additional geometric consequences of complex formation are a lengthening of the Si4−O12 bonds (by 0.05−0.06 Å) and Al1−Cl bonds (by 0.02−0.12 Å), especially for the chlorine eclipsed to the hydroxyl hydrogen. Again, the changes are larger for **10** than for **4** (Table S1). Elongation of the acceptor−ligand (A−L) bonds is one of the most pronounced geometrical changes noted by Hargittai and co-workers[58,60,61] in their investigations of the structural aspects of donor−acceptor complexes. When the donor molecule is ammonia, these researchers cite $n_N \rightarrow \sigma_{AL}^*$ and $\sigma_{NH} \rightarrow \sigma_{AL}^*$ hyperconjugative effects as one of two primary reasons for the bond elongation. The second reason cited is greater A−L/A−L repulsion due to the pyramidalization of the $AL_3$ geometry. The analogous hyperconjugation effects between the $n_{O12}$, $\sigma_{O12-H15}$, and $\sigma_{Al1-Cl}^*$ orbitals are also observed in this work for both **4** and **10** (Table 3).

*Transition States*. The structure of transition state **5** (reaction 7) indicates that the H15−Cl2 bond has been nearly completely formed at the transition state (Figure 4 and Table S1). The O12−H15 and Al1−Cl2 bonds have been only partially dissociated at the transition state, although the dissociation is considerably more advanced for the former bond. Upon examining the analogous interactions for transition state **8** (reaction 8), one finds that the bond breaking and forming processes are less complete (Figure 4 and Table S1). In short, transition state **5** is more productlike and transition state **8** is more reactantlike. For the reactions with the dimer substrate, comparison of transition

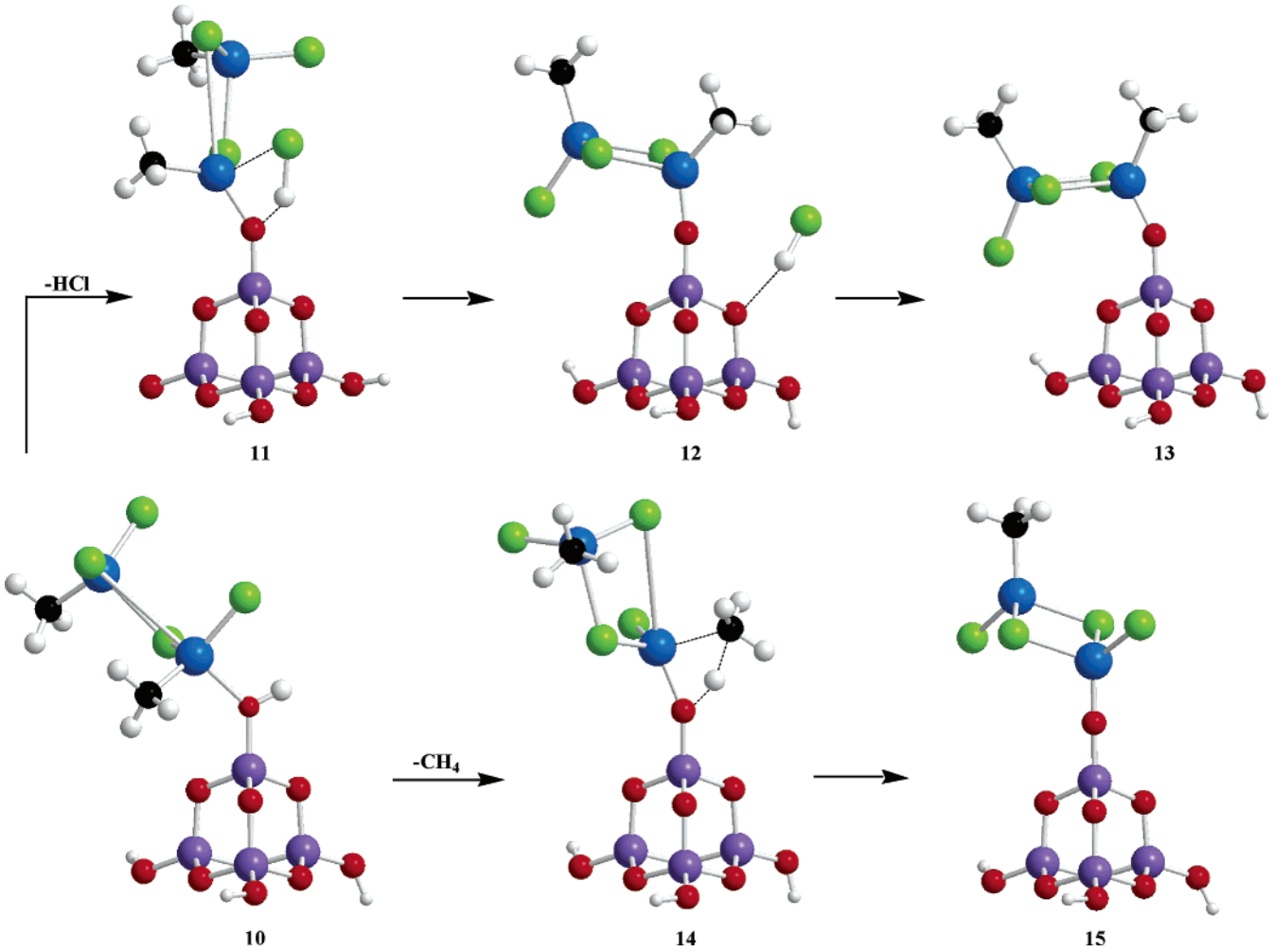


**Figure 5.** Stationary point structures of the two possible reaction pathways for the reaction of $Si_4O_6(OH)_4$ (**1**) with $Al_2Cl_4(CH_3)_2$ (**3**).

**TABLE 3: Computed Molecular Properties**[a]

| molecule | $q_{O12}$ | $q_{Al1}$ | $\Delta E^b$ |
|---|---|---|---|
| **1** | −1.164 | | |
| **2** | | 1.740 | |
| **3** | | 1.686 | |
| **4** | −1.203 | 1.753 | $n_{O12} \rightarrow p_{z,Al1}$, 241.9; $\sigma_{Si4-O12} \rightarrow p_{z,Al1}$, 59.45<br>$\sigma_{O12-H15} \rightarrow p_{z,Al1}$, 36.99; $n_{O12} \rightarrow \sigma^*_{Al1-Cl2}$, 24.81<br>$n_{O12} \rightarrow \sigma^*_{Al1-Cl3}$, 25.40; $\sigma_{O12-H15} \rightarrow \sigma^*_{Al1-Cl2}$, 4.94 |
| **5** | −1.382 | 1.856 | |
| **6** | | | $n_{Cl2} \rightarrow p_{z,Al1}$, 185.64; $n_{Cl2} \rightarrow \sigma^*_{Al1-O12}$, 25.36<br>$n_{Cl2} \rightarrow \sigma^*_{Al1-C4}$, 13.18; $\sigma_{H15-Cl2} \rightarrow p_{z,Al1}$, 9.75<br>$n_{O9} \rightarrow \sigma^*_{H15-Cl2}$, 54.56 |
| **7** | −1.422 | 1.965 | |
| **8** | −1.347 | 1.800 | |
| **9** | −1.425 | 1.905 | |
| **10** | −1.209 | 1.795 | $n_{O12} \rightarrow p_{z,Al1}$, 242.1; $\sigma_{Si4-O12} \rightarrow p_{z,Al1}$, 73.85<br>$\sigma_{O12-H15} \rightarrow p_{z,Al1}$, 42.47; $n_{O12} \rightarrow \sigma^*_{Al1-Cl2}$, 24.14<br>$n_{O12} \rightarrow \sigma^*_{Al1-Cl3}$, 33.39; $\sigma_{O12-H15} \rightarrow \sigma^*_{Al1-Cl2}$, 4.35 |
| **11** | −1.391 | 1.891 | |
| **12** | −1.425 | 1.930 | $n_{Cl2} \rightarrow \sigma^*_{Al1-O12}$, 3.18; $n_{Cl2} \rightarrow \sigma^*_{Al1-C4}$, 1.30<br>$n_{O9} \rightarrow \sigma^*_{H15-Cl2}$, 36.78 |
| **13** | −1.416 | 1.928 | |
| **14** | −1.355 | 1.842 | |
| **15** | −1.423 | 1.905 | |

[a] Energies are given in kilojoules per mole. Atom numbering is from Figure 1.

states **11** (reaction 9) and **14** (reaction 10) leads to the same conclusions (Figure 5 and Table S1).

Regardless of whether the reaction involves the monomer or dimer reactant, the more reactantlike transition state for the loss of $CH_4$ can be partially explained by the positions of the Cl2 and C4 atoms relative to the relevant H15 atom in the prereaction complexes. The placement of the Cl2 atom is more favorable than that of the C4 atom with respect to both the H15−O12−Al1−X dihedral angle and H15···X distance (see above). Thus, converting the prereaction complex into the transition state

**TABLE 4: Relative Thermochemical Data**[a]

| species | $\Delta(E + \text{ZPE})$ | $\Delta H_{298}$ | $\Delta S_{298}$ | $\Delta G_{298}$ |
|---|---|---|---|---|
| | Monomer Reaction: Loss of HCl | | | |
| $Si_4O_6(OH)_4$ (**1**) + $AlCl_2CH_3$ (**2**) | 0.0 | 0.0 | 0.0 | 0.0 |
| $Si_4O_6(OH)_4{-}AlCl_2CH_3$ (**4**) | −86.0 | −85.4 | −173.4 | −33.7 |
| TS1 (**5**) | −28.2 | −29.0 | −174.7 | 23.1 |
| $ClH\cdots Si_4O_7(OH)_3{-}AlClCH_3$ (**6**) | −62.5 | −61.4 | −171.1 | −10.4 |
| $Si_4O_7(OH)_3{-}AlClCH_3$ (**7**) + HCl | −21.7 | −19.2 | 12.1 | −22.8 |
| | Monomer Reaction: Loss of $CH_4$ | | | |
| TS2 (**8**) | −20.9 | −22.5 | −180.0 | 31.1 |
| $Si_4O_7(OH)_3{-}AlCl_2$ (**9**) + $CH_4$ | −167.0 | −164.5 | −22.8 | −157.7 |
| | Dimer Reaction: Loss of HCl | | | |
| $Si_4O_6(OH)_4$ (**1**) + $Al_2Cl_4(CH_3)_2$ (**3**) | 0.0 | 0.0 | 0.0 | 0.0 |
| $Si_4O_6(OH)_4{-}Al_2Cl_4(CH_3)_2$ (**10**) | −29.3 | −27.0 | −131.1 | 12.1 |
| TS3 (**11**) | 35.4 | 36.9 | −124.1 | 73.9 |
| $ClH\cdots Si_4O_7(OH)_3{-}Al_2Cl_3(CH_3)_2$ (**12**) | −50.1 | −46.8 | −122.1 | −10.4 |
| $Si_4O_7(OH)_3{-}Al_2Cl_3(CH_3)_2$ (**13**) + HCl | −32.3 | −30.4 | −19.1 | −24.7 |
| | Dimer Reaction: Loss of $CH_4$ | | | |
| TS4 (**14**) | 46.2 | 46.7 | −135.8 | 87.2 |
| $Si_4O_7(OH)_3{-}Al_2Cl_4(CH_3)$ (**15**) + $CH_4$ | −176.8 | −173.8 | −8.4 | −171.3 |

[a] $\Delta S_{298}$ values are given in joules/(kelvin·mole); all other values are given in kilojoules per mole.

requires considerably more reorientation of atoms for the loss of methane than for the loss of hydrochloric acid.

*Hydrogen-Bonded Complexes and Products*. In the hydrogen-bonded complexes **6** and **12**, the HCl product interacts with a siloxane oxygen adjacent to the modified silanol group (Figures 4 and 5). The longer O9···H15 distance (2.081 vs 1.969 Å) and shorter H15−Cl2 distance (1.273 vs 1.283 Å) in **12** indicate that the hydrogen bond is weaker for the dimer system. This conclusion is supported by the relative magnitudes of the complex dissociation energies (Table 4) and the $\Delta E^{(2)}(n_{O9} \rightarrow \sigma_{H15-Cl2}^*)$ values (Table 3) for **6** and **12**. As a point of reference, at the same level of calculation the complex $H_2O\cdots HCl$ has an O···H bond length of 1.975 Å and a H−Cl bond length of 1.277 Å.[62] On the basis of the bond length data, the interactions in $H_2O\cdots HCl$ and **6** have similar strengths.

Another important difference in the two hydrogen-bonded complexes is the distance between the Cl of the hydrochloric acid and the modified Al atom, which is 2.785 Å for **6** and 4.090 Å for **12**. The shorter Al1···Cl2 distance and empty $p_z$ orbital of Al1 in the former system allow an overlap between the $n_{Cl2}$ and $p_{z,Al1}$ orbitals that is absent in the latter system (Table 3). The $\sigma_{H15-Cl2} \rightarrow p_{z,Al1}$, $n_{Cl2} \rightarrow \sigma_{Al1-O12}^*$, and $n_{Cl2} \rightarrow \sigma_{Al-C4}^*$ hyperconjugations also contribute more significantly to the charge-transfer process in **6** than in **12**. These hyperconjugative effects help to elucidate the difference in the complexation energies of **6** and **12**. A second consequence of these effects is that the hydrochloric acid is more favorably aligned for reverse reaction **6** → **4** to proceed than for reverse reaction **12** → **10**.

With the exception of product **13**, the Si4−O12−Al1 bond is more linear in the product complex than it is in any other structure along a given reaction sequence (Figures 4 and 5, Table S1). Bending this angle in **13** provides a (very) weak interaction between the unbridged Cl9 atom and a silanol group. As the Si4−O12−Al1 angles along a reaction sequence become more linear, the charge separation between O12 and Al1 increases (Table 3), indicating that the ionic character of the bonds is also increasing.

**D. Reaction Energetics: Computational.** *Monomer vs Dimer Reactant Pathways.* Consider first the $\Delta(E + \text{ZPE})$ entries in Table 4. Both prereaction complexes are stabilized compared to reactants, but **4** is stabilized by some 50 kJ/mol more than **10**. The structural data discussed in the previous section indicate that the donor−acceptor bond in **10** is slightly stronger than that in **4**. Thus, the difference in stability is primarily due to the energy cost of breaking the Al1−Cl10 bond when **10** is formed. The height of the transition state above the prereaction complex is 55−65 kJ/mol for the monomer reactant pathways (reactions 7 and 8) and about 10 kJ/mol higher for the corresponding dimer reactant pathways (reactions 9 and 10). In net, the transition-state energies lie below that of the reactants for the monomer pathways but well above that of the reactants for the dimer pathways.

As a result of the stronger Al1···Cl2−H15···O9 interactions for the monomer (see structural details for the hydrogen-bonded complexes above), hydrogen-bonded complex **6** (reaction 7) is about 10 kJ/mol more stable than hydrogen-bonded complex **12** (reaction 9). Nevertheless, the activation barrier for reverse reaction **12** → **10** is nearly 3 times higher (∼85 kJ/mol) than the barrier for reverse reaction **6** → **4** (∼34 kJ/mol, Figures 4 and 5). Overall, each of the four reactions is exothermic, but ca. 10 kJ/mol more heat is evolved by the reactions with $Al_2Cl_4(CH_3)_2$ than by those with $AlCl_2CH_3$.

The values of $\Delta(E + \text{ZPE})$ and $\Delta H$ are nearly identical for each step along the four reaction pathways (Table 4, eqs 11 and 12). For reactions 7 and 8, the $\Delta S$ terms for the prereaction complex, transition state, and hydrogen-bonded complex relative to reactants are nearly constant at about −170 J/(K mol). The analogous terms for the systems involved in reactions 9 and 10 have nearly constant values of about −125 J/(K mol). For prereaction complex **10** and transition states **5** and **8**, the magnitude of the $T\Delta S$ contribution is sufficiently large to reverse the sign of $\Delta G$ with respect to that of $\Delta H$. As a result, these systems now lie uphill in energy compared to reactants. The only other difference in the trends for $\Delta G$ and $\Delta H$ is that conversion of the hydrogen-bonded complexes to products is endothermic but exergonic (reactions 7 and 9).

*Loss of HCl vs Loss of $CH_4$*. The $\Delta(E + \text{ZPE})$ values in Table 4 indicate that the activation barrier for the loss of HCl (reactions 7 and 9) is 5−10 kJ/mol lower than that for the loss of $CH_4$ (reactions 8 and 10). These relative energies are consistent with the more favorable Cl···H vs $H_3C\cdots H$ alignment in the prereaction complexes (Figures 4 and 5). In contrast, the overall decrease in free energy is 135−145 kJ/mol greater for the loss of $CH_4$ than for the loss of HCl. In each case the larger number applies to the reaction with the dimer reactant. Since the transition states for reactions 8 and 10 are more reactantlike

whereas those for reactions 7 and 9 are more productlike, each of these reactions obeys the Leffler−Hammond postulate.[63,64]

Regardless of whether the reactant is **2** or **3**, the calculational results suggest that formation of HCl is kinetically favored but formation of $CH_4$ is thermodynamically favored. These results are congruous with the experimentally observed formation of $CH_4$ if the conversion of prereaction complex to hydrogen-bonded complex is reversible for the sequences involving HCl. The overall reaction is therefore thermodynamically rather than kinetically driven. One of the factors that differentiates monomer reaction 7 from dimer reaction 9 is that this conversion is unlikely to be reversible for the latter reaction. When this irreversibility is coupled with the dimer's less stable prereaction complex and larger energies of forward activation, the computational data support $AlCl_2CH_3$ **2** as the preferred reactant. Moreover, low activation barriers are required to rationalize the experimentally observed reaction rates for similar reactions.[7]

Of course, the energies of activation are sufficiently close in magnitude (Table 4) that higher-level calculations could reverse the kinetically favored pathway. Although replacing the $CH_3$ ligand with $CH_2CH_3$ would partially offset such a reversal, it is possible that loss of alkane is both kinetically and thermodynamically favorable.

*Solvation Effects*. Accounting for solvation effects on the energy barriers of the $AlCl_2CH_3$ reactions demonstrates that the nonpolar solvents *n*-heptane and toluene inhibit both reactions slightly by enhancing the polarity of the prereaction complex more than that of either transition state. The change in activation energy $\Delta E^{\ddagger}$ due to solvation depends only minimally on solvent type. For the process **4** → **6** (loss of HCl), $\Delta E^{\ddagger}$ is 8 kJ/mol for *n*-heptane and 10 kJ/mol for toluene. For the process **4** → **8** (loss of $CH_4$), $\Delta E^{\ddagger}$ is 5 and 7 kJ/mol, respectively. The small value of $\delta\Delta E^{\ddagger} = 2$ kJ/mol for these two solvents is consistent with the experimental observation that there is no observed difference in the reaction in the two solvents.

## Conclusions

Experimental and computational studies of the reactions of alkylaluminum chlorides with silica gels that have undergone various forms of pretreatment have been described. The silica gel pretreatments alter surface chemistry as a means to understand how alkylaluminum compounds react with different surface groups. Infrared spectroscopic studies of the silica gels after reaction indicate that all non-hydrogen-bonded silanols are reacted by all of the reactants under the conditions studied. Elemental analysis data shows that hydrogen-bonded silanols and siloxanes are also reacted to similar extents by all of the alkylaluminum compounds. One noteworthy exception is the reaction of ethylaluminum dichloride with HMDZ-modified silica gel. The aluminum concentration (millimoles of Al/gram of silica) of this modified silica gel is approximately twice that of the other ethylaluminum compounds reacted with HMDZ-silica gel.

On the basis of experimental infrared results it is believed that the alkylaluminum chlorides preferentially react by Al−C bond cleavage as opposed to Al−Cl bond cleavage. It is therefore believed that ethylaluminum dichloride reacts with a single hydrogen-bonded silanol to form a surface $Si-O-AlCl_2$ linkage. In contrast, diethylaluminum chloride and triethylaluminum react in a 1:2 Al:SiOH ratio; with diethylaluminum chloride reacting to form a surface $(Si-O)_2-AlCl$ surface species. This latter reaction scheme is analogous to earlier studies of reactions of $TiCl_4$[16] and dibutylmagnesium[17] with HMDZ-modified silica gel surfaces. This explains the 2-fold increase in aluminum content of EADC-reacted HMDZ-modified silica gel and provides a means to vary the surface bonding of silica gels modified with AlCl groups.

Quantum chemical ab initio studies of the cluster $Si_4O_6(OH)_4$ as a model to study the reaction of monomeric and dimeric methylaluminum dichloride with a silica silanol are utilized to support the experimental results and to provide insights into the energetics of these reactions. Comparison of the PES of monomer and dimer indicates that the energetics favor monomer reaction. This is consistent with our conclusions from the experimental results. The energy cost in the dimer reaction is primarily from cleavage of a bridged Al−Cl bond upon adsorption. This does not occur when the monomer adsorbs.

Computational studies of the PES for the two reaction pathways of methylaluminum dichloride reacting with $Si_4O_6(OH)_4$ resulting from cleavage of either an Al−Cl or Al−C bond support the experimental conclusion that the reaction occurs preferentially by Al−C bond cleavage. For the monomer reaction, the calculated activation energy of Al−Cl bond cleavage is 23.1 kJ/mol, whereas Al−C bond cleavage activation energy is 31.1 kJ/mol. This indicates that Al−Cl bond breaking is kinetically favored. However, the overall free energy change for the two reaction pathways indicates that the Al−Cl bond breaking pathway is −22.8 kJ/mol, whereas the Al−C bond breaking pathway is −157.7 kJ/mol. This, along with the result that the Al−Cl bond breaking pathway is thermodynamically reversible, indicates that these reactions proceed under thermodynamic control. Taking into account solvation effects in the calculations, since the reactions were experimentally carried out in hexane, only slightly alters the computed energetics of these reactions.

**Acknowledgment.** Assistance from Equistar Chemicals, LP, in obtaining the ICP elemental analysis results as well as the silanol content data is gratefully acknowledged.

**Supporting Information Available:** Table S1 giving selected bond lengths, bond angles, and dihedral angles for molecules **1**−**15**, HCl, and $CH_4$. This material is available free of charge via the Internet at http://pubs.acs.org.

## References and Notes

(1) Yates, D. J. C.; Dembinski, G. W.; Kroll, W. R.; Elliott, J. J. *J. Phys. Chem.* **1969**, *73*, 911.
(2) Peglar, R. J.; Hambleton, F. H.; Hockey, J. A. *J. Catal.* **1971**, *20*, 309.
(3) Hambleton, F. H.; Hockey, J. A. *J. Catal.* **1971**, *20*, 321.
(4) Morrow, B. A.; Hardin, A. H. *J. Phys. Chem.* **1979**, *83*, 3135.
(5) Low, M. J. D.; Severdia, A. G.; Chan, J. *J. Catal.* **1981**, *69*, 384.
(6) Kinney, J. B.; Staley, R. H. *J. Phys. Chem.* **1983**, *87*, 3735.
(7) Morrow, B. A.; McFarlan, A. J. *J. Non-Cryst. Solids* **1990**, *120*, 61−71.
(8) Bartram, M. E.; Michalske, T. A.; Rogers, J. W., Jr. *J. Phys. Chem.* **1991**, *95*, 4453.
(9) Kratochvila, J.; Kadle, Z.; Kazda, A.; Salajka, Z. *J. Non-Cryst. Solids* **1992**, *143*, 14.
(10) Molotovschikova, M. B.; Dodonov, B. A.; Lysenko, G. N.; Ignatov, S. K.; Razuvaev, A. G. *Russ. Chem. Bull.* **1995**, *44*, 1827.
(11) Sindelar, P.; Matula, P.; Holecek, J. *J. Polym. Sci. A: Polym. Chem.* **1996**, *34*, 2163.
(12) Anwander, R.; Palm, C.; Groeger, O.; Engelhardt, G. *Organometallics* **1998**, *17*, 2027.
(13) Puurunen, R.; Root, A.; Haukka, S.; Iiskola, E. I.; Linblad, M.; Krause, A. O. I. *J. Phys. Chem. B* **2000**, *104*, 6599.
(14) Tao, T.; Maciel, G. E. *J. Am. Chem. Soc.* **2000**, *122*, 3118.
(15) Puurunen, R. C.; Root, A.; Saru, P.; Viitanen, M. M.; Brongersma, H. H.; Lindblad, M.; Krause, A. O. I. *Chem. Mater.* **2002**, *14*, 720.
(16) Blitz, J. P. *Colloids Surf.* **1992**, *63*, 11.
(17) Blitz, J. P.; Meverden, C. C.; Diebel, R. K. *Langmuir* **1998**, *14*, 1122.

(18) Ellingsen, D. G.; Dahl, I. M.; Ellestad, O. H. *J. Mol. Catal.* **1980**, *9*, 423.
(19) Dahl, I. M.; Halvorsen, S.; Ellingsen, D. G. *J. Mol. Catal.* **1986**, *35*, 55.
(20) Salajka, Z.; Kratochvila, J.; Havrik, O.; Kazda, A.; Gheorghiu, M. *J. Polym. Sci. A: Polym. Chem.* **1990**, *28*, 1651.
(21) Pullukat, T. J.; Hoff, R. E. U.S. Patent 4,530,912, 1985.
(22) Murthy, R. S. S.; Leyden, D. E. *Anal. Chem.* **1986**, *58*, 1228.
(23) Murthy, R. S. S.; Blitz, J. P.; Leyden, D. E. *Anal. Chem.* **1986**, *58*, 3167.
(24) Frisch, M. J.; Trucks, G. W.; Schlegel, H. B.; Scuseria, G. E.; Robb, M. A.; Cheeseman, J. R.; Montgomery, J. A., Jr.; Vreven, T.; Kudin, K. N.; Burant, J. C.; Millam, J. M.; Iyengar, S. S.; Tomasi, J.; Barone, V.; Mennucci, B.; Cossi, M.; Scalmani, G.; Rega, N.; Petersson, G. A.; Nakatsuji, H.; Hada, M.; Ehara, M.; Toyota, K.; Fukuda, R.; Hasegawa, J.; Ishida, M.; Nakajima, T.; Honda, Y.; Kitao, O.; Nakai, H.; Klene, M.; Li, X.; Knox, J. E.; Hratchian, H. P.; Cross, J. B.; Adamo, C.; Jaramillo, J.; Gomperts, R.; Stratmann, R. E.; Yazyev, O.; Austin, A. J.; Cammi, R.; Pomelli, C.; Ochterski, J. W.; Ayala, P. Y.; Morokuma, K.; Voth, G. A.; Salvador, P.; Dannenberg, J. J.; Zakrzewski, V. G.; Dapprich, S.; Daniels, A. D.; Strain, M. C.; Farkas, O.; Malick, D. K.; Rabuck, A. D.; Raghavachari, K.; Foresman, J. B.; Ortiz, J. V.; Cui, Q.; Baboul, A. G.; Clifford, S.; Cioslowski, J.; Stefanov, B. B.; Liu, G.; Liashenko, A.; Piskorz, P.; Komaromi, I.; Martin, R. L.; Fox, D. J.; Keith, T.; Al-Laham, M. A.; Peng, C. Y.; Nanayakkara, A.; Challacombe, M.; Gill, P. M. W.; Johnson, B.; Chen, W.; Wong, M. W.; Gonzalez, C.; Pople, J. A. *Gaussian 98*, Revision A.1; Gaussian, Inc.: Pittsburgh, PA, 1998.
(25) Hehre, W. J.; Radom, L.; Schleyer, P. v. R.; Pople, J. A. *Ab Initio Molecular Orbital Theory*; Wiley: New York, 1986.
(26) Ugliengo, P.; Saunders, V.; Garrone, E. *J. Phys. Chem.* **1990**, *94*, 2260−2267.
(27) Ugliengo, P.; Saunders, V. R.; Garrone, E. *J. Phys. Chem.* **1989**, *93*, 5210−5215.
(28) Catti, M.; Civalleri, B.; Ugliengo, P. *J. Phys. Chem. B* **2000**, *104*, 7259−7265.
(29) Civalleri, B.; Casassa, S.; Garrone, E.; Pisani, C.; Ugliengo, P. *J. Phys. Chem. B* **1999**, *103*, 2165−2171.
(30) Garrone, E.; Barbaglia, A.; Onida, B.; Civalleri, B.; Ugliengo, P. *Phys. Chem. Chem. Phys.* **1999**, *1*, 4649−4654.
(31) Ugliengo, P.; Garrone, E.; Ferrari, A. M.; Zecchina, A.; Arean, C. *J. Phys. Chem. B* **1999**, *103*, 4839−4846.
(32) Ugliengo, P.; Civalleri, B.; Dovesi, R.; Zicovich-Wilson, C. M. *Phys. Chem. Chem. Phys.* **1999**, *1*, 545−554.
(33) Civalleri, B.; Garrone, E.; Ugliengo, P. *J. Phys. Chem. B* **1998**, *102*, 2373−2382.
(34) Ugliengo, P.; Ferrari, A. M.; Zecchina, A.; Garrone, E. *J. Phys. Chem.* **1996**, *100*, 3632−3645.
(35) Ferrari, A. M.; Ugliengo, P.; Garrone, E. *J. Chem. Phys.* **1996**, *105*, 4129−4139.
(36) Garrone, E.; Ugliengo, P.; Ghiotti, G.; Borello, E.; Saunders, V. R. *Spectrochim. Acta Part A* **1993**, *49*, 1221−1234.
(37) Ferrari, A. M.; Ugliengo, P.; Garrone, E. *J. Phys. Chem.* **1993**, *97*, 2671−2676.
(38) Garrone, E.; Kazansky, V. B.; Kustov, L. M.; Sauer, J.; Senchenya, I. N.; Ugliengo, P. *J. Phys. Chem.* **1992**, *96*, 1040−1045.
(39) Civalleri, B.; Casassa, S.; Garrone, E.; Pisani, C.; Ugliengo, P. *J. Phys. Chem B* **1999**, *103*, 2165.
(40) Civalleri, B.; Zicovich-Wilson, C. M.; Ugliengo, P.; Saunders, V. R.; Dovesi, R. *Chem. Phys. Lett.* **1998**, *292*, 394−402.
(41) Pelmenschikov, A. G.; Morosi, G.; Gamba, A. *J. Phys. Chem. A* **1997**, *101*, 1178−1187.
(42) Civalleri, B.; Garrone, E.; Ugliengo, P. *Langmuir* **1999**, *15*, 5829−5835.
(43) Molotovshchikova, M. B.; Dodonov, V. A.; Lysenko, G. N.; Ignatov, S. K.; Razuvaev, A. G. *Russ. Chem. Bull.* **1995**, *44*, 1827−1831.
(44) Glendening, E. D.; Reed, A. E.; Carpenter, J. E.; Weinhold, F. NBO Version 3.1.
(45) Mulliken, R. S. *J. Chem. Phys.* **1955**, *23*, 1833, 1841, 2338, and 2343.
(46) (a) Besler, B. H.; Merz, K. M., Jr.; Kollman, P. A. *J. Comput. Chem.* **1990**, *11*, 431. (b) Singh, U. C.; Kollman, P. A. *J. Comput. Chem.* **1984**, *5*, 129.
(47) Xidos, J. D.; Li, J.; Zhu, T.; Hawkins, G. D.; Thompson, J. D.; Chuang, Y.-Y.; Fast, P. L.; Liotard, D. A.; Rinaldi, D.; Cramer, C. J.; Truhlar, D. G. *GAMESOL-version 3.1*; University of Minnesota: Minneapolis, MN, 2002; based on the General Atomic and Molecular Electronic Structure System (GAMESS) as described in Schmidt, M. W.; Baldridge, K. K.; Boatz, J. A.; Elbert, S. T.; Gordon, M. S.; Jensen, J. H.; Koseki, S.; Matsunaga, N.; Nguyen, K. A.; Su, S. J.; Windus, T. L.; Dupuis, M.; Montgomery, J. A. *J. Comput. Chem.* **1993**, *14*, 1347.
(48) Smith, M. B. *J. Organomet. Chem.* **1974**, *70*, 13.
(49) Rottler, R.; Kreiter, C. G.; Fink, G. *Z. Naturforsch.* **1976**, *31b*, 730.
(50) Fraile, J. M.; Garcia, J. I.; Mayoral, J. A.; Pires, E. *J. Mol. Catal.* **1997**, *119*, 95.
(51) Kytokivi, A.; Haukka, S. *J. Phys. Chem. B* **1997**, *101*, 10365.
(52) Drago, R. S.; Petrosius, S. C.; Kaufman, P. B. *J. Mol. Catal.* **1994**, *89*, 317.
(53) Sato, S.; Maciel, G. E. *J. Mol. Catal. A: Chem.* **1995**, *101*, 153.
(54) An experimental comparison of $AlCl_3$ reactivity was not accomplished due to the low solubility of $AlCl_3$ in hexanes.
(55) Reed, A. E.; Curtiss, L. A.; Weinhold, F. *Chem. Rev.* **1988**, *88*, 899.
(56) Kudo, T.; Gordon, M. S. *J. Phys. Chem. A* **2002**, *106*, 11347−11353.
(57) Xu, T.; Kob, N.; Drago, R. S.; Nicholas, J. B.; Haw, J. F. *J. Am. Chem. Soc.* **1997**, *119*, 12231−12239.
(58) Horvth, V.; Kovcs, A.; Hargittai, I. *J. Phys. Chem. A* **2003**, *107*, 1197−1202. Analogous, but considerably larger, intermolecular charge transfers and second-order perturbation energies were reported in this MP2/6-311+G(2df,p) study of $AL_3NH_3$ complexes, where A = B, Al, or Ga and L = H or Cl. For example, for $AlCl_3NH_3$ the $E^{(2)}(n_N \rightarrow p_{z,Al})$ value is 600.0 kJ/mol and the intermolecular charge transfer is 0.187e. [The $\Delta E^{(2)}$ values were computed from HF/6-311+G(2df,p) single-point calculations on the MP2/ 6-311+G(2df,p) geometries.]
(59) Fraile, J. M.; Garca, J. I.; Mayoral, J. A.; Pires, E. *J. Mol. Catal. A* **1997**, *119*, 95−103.
(60) Hargittai, M.; Hargittai, I. *J. Mol. Struct.* **1977**, *39*, 79.
(61) Hargittai, M.; Hargittai, I. *The Molecular Geometries of Coordination Compounds in the Vapor Phase*; Elsevier: Amsterdam, 1977; pp 68−71.
(62) Zvereva, N. A. *J. Struct. Chem.* **2001**, *42*, 730−738.
(63) Hammond, G. S. *J. Am. Chem. Soc.* **1955**, *77*, 334.
(64) Leffler, J. E. *Science* **1953**, *117*, 340.